Supporting Information

Hierarchical Porous Catalytic Pyrolysis Char Derived from Oily Sludge for Enhanced Adsorption

Dong Han[a, b], Xiaoyu Li[a*, b], Zhiqiang Gong[c], Lanyue Jiang[a], Zhenbo Wang[b*], Peikun Liu[a]

[a] College of Mechanical and Electronic Engineering, Shandong University of Science and Technology, Qingdao 266590, China. E-mail address: lixy2018@sdust.edu.cn.

[b] College of New Energy, China University of Petroleum(East China), Qingdao 266580, China. E-mail address: dxl437@sina.com.

[c] State Grid Shandong Electric Power Research Institute, Jinan 250003, China.

Explanations and formulas for isotherm models

The Langmuir model assumes that the adsorbent surface is homogeneous, and the adsorption energy is the same on the surface. The adsorption is monolayer adsorption. When the adsorption equilibrium reached, the number of molecules entering the adsorption site is equal to the number of molecules leaving in unit time, in other words, the adsorption rate is equal to the desorption rate [1]. The linear formula of the Langmuir model is expressed as follows:

$$\frac{c_e}{q_e} = \frac{1}{q_m K_L} + \frac{c_e}{q_m}$$

Where, q_e is the equilibrium adsorption capacity (mg/g), c_e is the equilibrium concentration of the dye solution (mg/L), q_m is the saturated adsorption capacity (mg/g) and K_L is the Langmuir constant (L/mg).

The dimensionless constant R_L normally known as separation factor expressed as follows:

$$R_L = \frac{1}{1 + K_L c_e}$$

When $R_L>1$, $R_L=1$, $0<R_L<1$, and $R_L=0$, the adsorption process is predicted to be non-favorable, linear, favorable and non-reversible, respectively [2].

The Freundlich model is an empirical formula without any assumptions, because the constants in the formula have no definite physical meaning [3]. The linear formula of

Freundlich model is shown as follows:

$$\ln q_e = \ln K_F + \frac{1}{n} \ln c_e$$

Where, K_F is the Freundlich constant [(mg/g)(L/mg)$^{1/n}$] related to the adsorption interaction and the adsorption capacity, n is a constant related to the adsorption intensity.

Explanations and formulas for kinetic models:

The linear formula of Pseudo-first-order model is shown as follows:

$$\ln(q_{e.\exp} - q_t) = \ln q_{e.cal} - k_1 t$$

Where, $q_{e.exp}$ is the experimental equilibrium adsorption capacity (mg/g), $q_{e.cal}$ is the calculated equilibrium adsorption capacity (mg/g), q_t is the adsorption capacity at time t (mg/g), k_1 is the Pseudo-first-order rate constant (min^{-1}), t is the pre-set time intervals (min).

The linear formula of Pseudo-second-order model is shown as follows:

$$\frac{t}{q_t} = \frac{1}{k_2 q_{e.cal}^2} + \frac{1}{q_{e.cal}} t$$

Where, k_2 is the Pseudo-second-order rate constant (g mg^{-1}min^{-1}).

Table S1 Characteristics of the OS used in this paper.

	Ultimate analysis					
element	C	H	O	N	S	Si
wt%	16.38	4.25	8.91	0.32	2.34	20.47
	Proximate analysis					
component	moisture	Volatile matter	ash	fixed carbon		
wt%	16.61	27.38	51.19	4.82		

Table S2 Fit summary of sequential model.

Sequential Model Sum of Squares						
Source	**Sum of squares**	**DF**	**Mean square**	**F-value**	**Prob>F**	
Mean vs Total	7.337E+005	1	7.337E+005			
Linear vs Mean	4707.93	3	1569.31	0.30	0.8268	
2FI vs Linear	3460.47	3	1153.49	0.18	0.9096	
Quadratic vs 2FI	65138.26	3	21712.75	2798.24	<0.0001	Suggested
Cubic vs Quadratic	10.76	3	3.59	0.33	0.8058	Aliased
Residual	43.56	4	10.89			
Total	8.071E+005	17	47476.00			
Lack of Fit tests						
Linear	68609.49	9	7623.28	700.08	<0.0001	
2FI	65149.02	6	10858.17	997.16	<0.0001	
Quadratic	10.76	3	3.59	0.33	0.8058	Suggested
Cubic	0.000	0				Aliased
Pure Error	43.56	4	10.89			
Model Summary Statistics						
source	Std. Dev.	R^2	R^2_{Adj}	R^2_{Pred}	PRESS	
Linear	72.67	0.0642	-0.1518	-0.3689	1.004E+005	
2FI	80.74	0.1113	-0.4218	-1.1132	1.550E+005	
Quadratic	2.79	0.9993	0.9983	0.9967	240.21	Suggested
Cubic	3.30	0.9994	0.9976			Aliased

Table S3 Analysis of variance (ANOVA) of the experimental results of RSM-BBD.

Source	Sum of squares	DF	Mean square	F-value	Prob>F	
Model	73306.66	9	8145.18	1049.72	<0.0001	**significant**
A	2778.14	1	2778.14	358.03	<0.0001	
B	1454.36	1	1454.36	187.43	<0.0001	
C	475.43	1	475.43	61.27	0.0001	
AB	308.79	1	308.79	39.80	0.0004	
AC	3149.79	1	3149.79	405.93	<0.0001	
BC	1.89	1	1.89	0.24	0.6372	
A^2	29270.40	1	29270.40	3772.24	<0.0001	
B^2	13766.04	1	13766.04	1774.11	<0.0001	
C^2	15500.73	1	15500.73	1997.66	<0.0001	
Residual	54.32	7	7.76			
Lack of Fit	10.76	3	3.59	0.33	0.8058	**not significant**
Pure Error	43.56	4	10.89			
Cor Total	73360.97	16				

Table S4 Statistical analysis for the quadratic model.

Statics	**Value**
Determination coefficient	0.9993
Adjusted determination coefficient	0.9983
Predicted determination coefficient	0.9967
Coefficient of variation (CV, %)	1.34
Adequate precision	92.892

Table S5

Adsorption isotherm parameters for MB adsorbed onto PC at different temperature.

Temperature (K)			**298**	**308**	**318**
Experimental q_e (mg/g)			282.69	305.51	322.89
Langmuir	q_m	mg/g	285.71	304.88	327.87
	K_L	L/mg	0.4094	0.3388	0.2032
	R_L		0.003~0.789	0.003~0.850	0.007~0.960
	R^2		0.9999	0.9999	0.9997
Freundlich	K_F	(mg/g)(L/mg)$^{1/n}$	178.95	183.06	193.37
	$1/n$		0.0844	0.0897	0.0905
	R^2		0.5635	0.6255	0.7153

Table S6

Adsorption kinetic parameters for MB adsorbed onto PC at different temperature.

Temperature (K)			298	308	318
Experimental $q_{e.exp}$ (mg/g)			282.69	305.51	322.89
Pseudo-first-order	$q_{e.cal}$	mg/g	275.03	299.62	308.34
	k_1	min^{-1}	5.0817	5.5723	5.1104
	R^2		0.9948	0.9972	0.9941
Pseudo-second-order	$q_{e.cal}$	mg/g	281.69	304.88	317.46
	k_2	g mg^{-1}min^{-1}	0.027	0.033	0.015
	R^2		0.9999	0.9999	0.9999

Table S7

Comparison of the MB adsorption capacity of various adsorbents

Adsorbents	adsorption capacity (mg g^{-1})	Reference
Oily sludge-based PC	**322.89**	**This work**
Nanoporous polymer	57.74	[4]
Hollow spherical sludge carbon	149	[5]
Cellulose nanocrystal-alginate hydrogel	256.41	[6]
Prosopis juliflora-based activated carbon	91	[7]
Corn stalk-based activated carbon	144	[8]
Eucalyptus sawdust-based activated carbon	178.57	[9]
Chitosan-clay composite	193.23	[10]
Wheat straw-based activated carbon	208	[11]
Wheat straw-based activated carbon	396.9	[12]

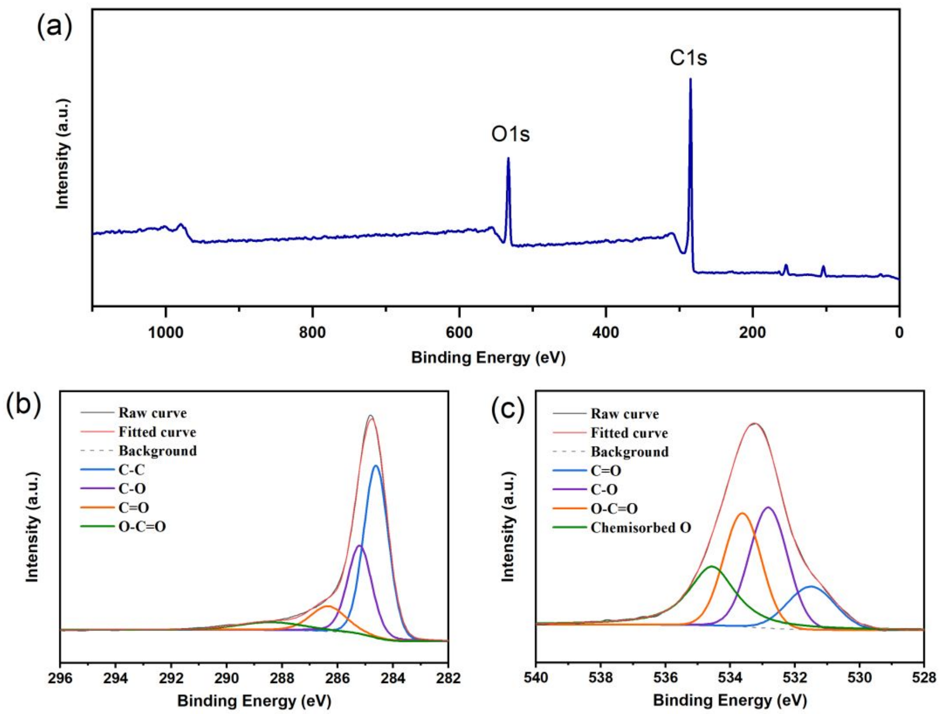

Figure S1. The XPS survey (a) and the high resolution of C1s (b) and O1s(c) spectrum of PC

As shown in Figure S1a, C1s, and O1s peaks can be observed clearly in the XPS survey. The high resolution C1s and O1s XPS spectra of PC are shown in Figure S1b and c, respectively. The C1s spectrum can be deconvoluted into four peaks which representing C-C (284.5 eV), C-O (285.7eV), C=O (287.3 eV) and C-C (288.7 eV), respectively [13]. The O1s spectrum can also be divided into four peaks which attributing to C=O (531.4 eV), C-O (532.3 eV), O-C=O (533.5 eV) and chemisorbed Oxygen (534.8 eV), respectively [14]. These O-containing functional group especially hydroxyl and carboxyl groups could generate electrostatic interactions and hydrogen bonding effect with MB ions, which promotes the adsorption performance of PC material.

Reference S

[1] S. P. D. Monte Blanco et al., Kinetic, equilibrium and thermodynamic phenomenological modeling of reactive dye adsorption onto polymeric adsorbent, *Chem. Eng. J.*, **2017**, *307*, 466-475.

[2] M. Iwan, B. Chao, Q. Lian, R. Subramaniam, M. Zappi, and D. Dianchen, Equilibrium , kinetic and thermodynamic studies for adsorption of BTEX onto Ordered Mesoporous Carbon (OMC), *J. Hazard. Mater.*, **2017**, *336*, 249-259.

[3] S. Xu, Y. Lv, X. Zeng, and D. Cao, ZIF-derived nitrogen-doped porous carbons as highly efficient adsorbents for removal of organic compounds from wastewater, *Chem. Eng. J.*, **2017**, *323*, 502-511.

[4] H. Su, W. Li, Y. Han, N. Liu, Magnetic carboxyl functional nanoporous polymer: synthesis, characterization and its application for methylene blue adsorption, *Sci. Rep.*, **2018**, *8*, 6506.

[5] Z.J. Wu, L.J. Kong, H. Hu, S.H. Tian, Y. Xiong, Adsorption Performance of Hollow Spherical Sludge Carbon Prepared from Sewage Sludge and Polystyrene Foam Wastes, *ACS Sustainable Chem. Eng.*, **2015**, *3*, 552-558.

[6] N. Mohammed, N. Grishkewich, R. Berry, K. Tam, Cellulose nanocrystal-alginate hydrogel beads as novel adsorbents for organic dyes in aqueous solutions, *Cellulose*, **2015**, *22*, 3725-3738.

[7] V. Nair, R. Vinu, Peroxide-assisted microwave activation of pyrolysis char for adsorption of dyes from wastewater, *Bioresour. Technol.*, **2016**, *216*, 511-519.

[8] Y.L. Li, Y.L. Li, L.P. Li, X.J. Shi, Z. Wang, Preparation and analysis of activated carbon from sewage sludge and corn stalk, *Adv Powder Technol*, **2016**, *27*, 684-691.

[9] L. Sun, D.M. Chen, S.G. Wan, Z.B. Yu, Performance, kinetics, and equilibrium of methylene blue adsorption on biochar derived from eucalyptus saw dust modified with citric, tartaric, and acetic acids, *Bioresour. Technol.*, **2015**, *198*, 300-308.

[10] M. Auta, B.H. Hameed, Chitosan-clay composite as highly effective and low-cost adsorbent for batch and fixed-bed adsorption of methylene blue, *Chem Eng J*, **2014**, *237*, 352-361.

[11] X.Y. Han, L. Chu, S.M. Liu, T.M. Chen, C. Ding, J.L. Yan, L.Q. Cui, G.X. Quan, Removal of Methylene Blue from Aqueous Solution using Porous Biochar Obtained by KOH Activation of Peanut Shell Biochar, *Bioresources*, **2015**, *10*, 2836-2849.

[12] R.P. Han, L.J. Zhang, C. Song, M.M. Zhang, H.M. Zhu, L.J. Zhang, Characterization of modified wheat straw, kinetic and equilibrium study about copper ion and methylene blue adsorption in batch mode, *Carbohyd Polym*, **2010**, *79*, 1140-1149.

[13] A.Y. Wang, K. Sun, L.P. Wu, P. Wu, W.C. Zeng, Z.M. Tian, Q.X. Huang, Co-carbonization of biomass and oily sludge to prepare sulfamethoxazole super-adsorbent materials, *Sci. Total Environ.,* **2020**, *698*, 134238.

[14] J.H. Zhou, Z.J. Sui, J. Zhu, P. Li, D. Chen, Y.C. Dai, W.K. Yuan, Characterization of

surface oxygen complexes on carbon nanofibers by TPD, XPS and FT-IR, *Carbon,* **2007**, *45*, 785–796